

Rate-Distortion Problems of the Poisson Process based on a Group-Theoretic Approach

Hui-An Shen, Stefan M. Moser, *Senior Member, IEEE*, and Jean-Pascal Pfister

Abstract—We study rate-distortion problems of a Poisson process using a group theoretic approach. By describing a realization of a Poisson point process with either point timings or inter-event (inter-point) intervals and by choosing appropriate distortion measures, we establish rate-distortion problems of a homogeneous Poisson process as ball- or sphere-covering problems for realizations of the hyperoctahedral group in \mathbb{R}^n . Specifically, the realizations we investigate are a hypercube and a hyperoctahedron. Thereby we unify three known rate-distortion problems of a Poisson process (with different distortion measures, but resulting in the same rate-distortion function) with the Laplacian- ℓ_1 rate-distortion problem.

Index Terms—Hyperoctahedral group, natural choice of distortion measure, Poisson point processes, rate-distortion function, sphere covering.

I. INTRODUCTION

In [1] we have studied the well-known geometric concept of *sphere covering*, which beautifully explains the rate-distortion problem for the Gaussian source under an ℓ_2 -distortion measure, and we have applied it to a Poisson process with an appropriately chosen distortion measure. We thereby succeeded in providing a new geometric proof of the converse to a rate-distortion theorem for a Poisson process.

In this work we would like to build on these insights and investigate more in details what underlying geometric structure is required for such a geometric proof. We will provide geometric, sphere-covering proofs to four known different rate-distortion problems: three rate-distortion problems for the Poisson process with different distortion measures, and one rate-distortion problem for the Laplacian- ℓ_1 source. Thereby we rely on group theory and some of its basic tools to connect these four different problems. Specifically, we use groups to describe certain symmetries inherent in the Poisson process.

The *permutation group*—the group that contains all possible permutations of n objects—is ideal to describe possible relabelings of event times of a realization of a homogeneous Poisson process (conditional on a given number of events), which is possible because the Poisson process is memoryless. So, we use the event timings to describe the Poisson process,

This work was supported by the Swiss National Science Foundation grants PP00P3_179060 (J.-P. P.) and 31003A_175644 (H.-A. S.). It was presented in part at the 2021 IEEE Information Theory Workshop. (*Corresponding author: Hui-An Shen.*)

Hui-An Shen and Jean-Pascal Pfister belong to the Theoretical Neuroscience Group, University of Bern, Switzerland, and are affiliated with the Institute of Neuroinformatics, University of Zurich and ETH Zurich, Switzerland (e-mail: {jeanpascal.pfister, huian.shen}@unibe.ch).

Stefan M. Moser is with the Signal and Information Processing Lab, ETH Zurich, Switzerland, and is affiliated with the Institute of Communications Engineering, National Yang Ming Chiao Tung University, Hsinchu, Taiwan (e-mail: moser@isi.ee.ethz.ch).

rely on the permutation group to set it into a geometric viewpoint, and—using point-covering distortion as a distortion measure—are then able to derive the point-covering rate-distortion function via the sphere-covering argument.

If, instead of the permutation group, its subgroup with only the identity permutation is used, the geometric picture fits to the case of the queueing rate-distortion problem. Note that both these problems correspond to ℓ_∞ -ball covering. They are explored in Section II.

Similarly, the *reflection group*—the group describing all possible reflections on the $(n - 1)$ -dimensional principle hyperplanes ($x_i = 0$) in the n -dimensional space—can be used to describe symmetries in the context of the inter-event intervals. In this case, we use the exponentially distributed inter-event intervals to describe the homogeneous Poisson process, rely on the subgroup of the reflection group containing only the identity element to obtain a geometric picture for it, and—in combination with a corresponding onesided ℓ_1 -distortion measure—are able to give the sphere-covering picture for the exponential onesided ℓ_1 -rate-distortion problem.

If we use the complete reflection group in combination with the ℓ_1 -distortion measure, we can geometrically represent the case of the Laplacian ℓ_1 -rate-distortion problem. So, these two problems are ℓ_1 -sphere-covering problems. They are explored in Section III.

These four different rate-distortion problems are briefly summarized in Figure 1. There the left column describes the event description and the right column the inter-event interval description of the process; and the rows distinguish whether the complete group or only its trivial subgroup is used as a geometric description of the source.

Note that a crucial aspect to these geometrical descriptions of the source and rate-distortion problem is an appropriate choice of the distortion measure. We introduce here the concept of a *natural choice* of distortion measure that guarantees that the distortion set around a codeword has a similar shape to the source set, leading to particularly easy formulations of the ball- or sphere-covering problem and rate-distortion function.

Finally in Section IV, we focus on the particular choice of permutation and reflection group as our main tool of geometric description. We show that they both can be derived from the so-called *hyperoctahedral group*, a group that describes all symmetries of a hypercube or of a regular hyperoctahedron; or more precisely, we will give construction of the hyperoctahedral group from the permutation group and the reflection group via the semidirect product. Thereby we demonstrate the connections between the hyperoctahedral group and the symmetries of a Poisson process.

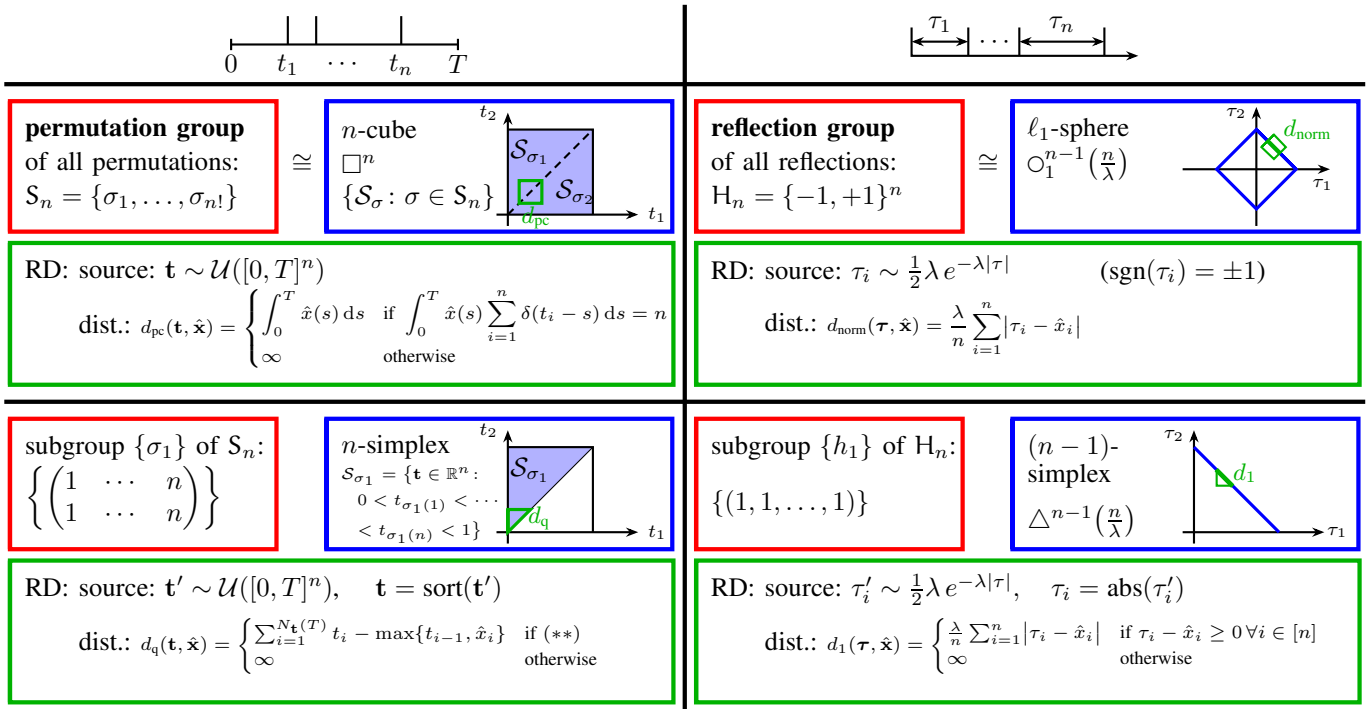


Fig. 1. Unification of four rate distortion problems. The left and right columns present the symmetries in the timing description (permutation group) and the interval description (reflection group), respectively. The upper and lower rows present the respective group and its subgroup. Each quadrant also illustrates its own rate-distortion problem with its source set (in the blue box) and its natural distortion measure “dist” (in the green box). In the left lower quadrant, we use Cauchy’s two-line notation for permutation to denote σ_1 ; and the (**) condition for finite distortion is $N_{\hat{\mathbf{x}}}(T) = N_{\mathbf{t}}(T)$ and $N_{\hat{\mathbf{x}}}(s) \geq N_{\mathbf{t}}(s) \forall s \in [0, T]$. Note that the blue lines on the right column illustrate the region where the source is concentrated (when $n \rightarrow \infty$).

Notation and Definitions

We use bold font \mathbf{x} to denote vectors; for sets we use a calligraphic font \mathcal{X} ; groups and group elements are denoted by the Euler font G ; and for a graph and its vertex and edge set, we use $\Gamma = (V, E)$.

By $\|\cdot\|_p$ we denote the ℓ_p -norm. Real metric and normed (linear) spaces are denoted by (X, d) and $(X, \|\cdot\|)$, respectively, the former with metric d and the latter with origin and norm $\|\cdot\|$. Sometimes we do not specify the metric or norm and only write X . In particular, the n -dimensional Euclidean space $(\mathbb{R}^n, \|\cdot\|_2)$ is denoted by E_n . We define

$$[n] \triangleq \{1, 2, \dots, n\}. \quad (1)$$

For $r > 0$,

$$\mathcal{O}_1^{n-1}(r) \triangleq \left\{ \mathbf{x} \in \mathbb{R}^n : \sum_{i=1}^n |x_i| = r \right\} \quad (2)$$

denotes the ℓ_1 -sphere of radius r . Its first-orthant (“hyper-surface”) $(n-1)$ -simplex is given as

$$\Delta^{n-1}(r) \triangleq \left\{ \mathbf{x} \in \mathbb{R}^n : \sum_{i=1}^n x_i = r, x_i \geq 0 \forall i \in [n] \right\}. \quad (3)$$

Furthermore, we define the n -dimensional unit-(hyper)cube $\square^n \triangleq [0, 1]^n$. We define \diamond^n to be the n -dimensional regular (hyper)octahedron with vertices $\{\pm \mathbf{e}_1, \pm \mathbf{e}_2, \dots, \pm \mathbf{e}_n\}$, where $\{\mathbf{e}_i\}_{i \in [n]}$ is an orthonormal basis of E_n .

We define the *permutation group* as the set of all permutations σ_i on n objects,

$$S_n \triangleq \{\sigma_1, \dots, \sigma_n!\}, \quad (4)$$

with composition “ \circ ” as group operation. Its identity element $e_{S_n} = \sigma_1$ is the identity mapping.

Remark 1: We are aware that in the literature this group is usually called “the symmetric group”, while the term “permutation group” is used for subgroups of S_n . However, in order to make a more clear distinction between S_n and the group of symmetries introduced later, we have decided to avoid the name “symmetric group”.

The *reflection group* H_n is defined as the n -fold direct product of $H \triangleq \{+1, -1\}$,

$$H_n \triangleq \{+1, -1\}^n, \quad (5)$$

with regular multiplication “ \cdot ” as group operation.

A *group isomorphism* between two groups $(G, *)$ and (H, \circ) is a bijective mapping $\varphi: G \rightarrow H$ such that

$$\varphi(g * g') = \varphi(g) \circ \varphi(g'), \quad \forall g, g' \in G. \quad (6)$$

Two groups G and H are *isomorphic*, written as $G \cong H$, if there exists a group isomorphism between them.

By vol_n we denote the n -dimensional Lebesgue measure. The logarithm $\log(\cdot)$ is to base 2; $\text{cl}(\cdot)$ denotes the closure of a set; $\text{conv}(\cdot)$ denotes the convex hull of a set of points; and $\mathbb{1}\{\text{statement}\}$ represents the indicator function, which equals 1 if the statement holds true and 0 otherwise.

II. RATE DISTORTION AND ℓ_∞ -BALL COVERING FOR THE HOMOGENEOUS POISSON PROCESS

A. The Hypercube and the Permutation Group

Each realization of a homogeneous Poisson point process over the duration $[0, T]$ has some number of points n and can thus be described by an n -tuple (t_1, t_2, \dots, t_n) where $t_1 < t_2 < \dots < t_n$. For convenience, we also define $t_0 \triangleq 0$.

Considering all permutations of each n -tuple and without loss of generality setting $T = 1$, the (closure of the) n -tuples and their permutations form a unit n -cube \square^n . We will next associate this cube with a group denoted G_n^{perm} .

To that goal, for any permutation $\sigma \in S_n$, we define the (“hypervolume”) n -simplex as

$$\mathcal{S}_\sigma \triangleq \{\mathbf{t} \in \mathbb{R}^n : 0 < t_{\sigma(1)} < t_{\sigma(2)} < \dots < t_{\sigma(n)} < 1\}. \quad (7)$$

Note that this n -simplex \mathcal{S}_σ “triangulates” the n -cube \square^n , and that the closure of the union of all these n -simplices forms the n -cube \square^n (compare also with left upper quadrant of Figure 1).

Definition 2: We define

$$G_n^{\text{perm}} \triangleq \{\mathcal{S}_\sigma : \sigma \in S_n\} \quad (8)$$

to be the associated group of the hypercube, where its group operation “ $*$ ” is defined by means of the group operation “ \circ ” of S_n :

$$\mathcal{S}_{\sigma_i} * \mathcal{S}_{\sigma_j} \triangleq \mathcal{S}_{\sigma_i \circ \sigma_j}. \quad (9)$$

Note that the collection of ordered n -tuples describing a homogeneous Poisson process is a subgroup of G_n^{perm} . Moreover, note that G_n^{perm} is, by definition, isomorphic to S_n .

Proposition 3: The mapping $\varphi_p: S_n \rightarrow G_n^{\text{perm}}$, $\sigma \mapsto \mathcal{S}_\sigma$ is an isomorphism.

Remark 4: Because of this isomorphism we henceforth also refer to G_n^{perm} as the permutation group.

From Proposition 3 we immediately get the identity element of G_n^{perm} :

$$\begin{aligned} \mathbf{e}_{G_n^{\text{perm}}} &= \varphi_p(\mathbf{e}_{S_n}) = \mathcal{S}_{\sigma_1} \\ &= \{\mathbf{t} \in \mathbb{R}^n : 0 < t_1 < t_2 < \dots < t_n < 1\}. \end{aligned} \quad (10)$$

Thus, the subgroup $\{\mathbf{e}_{G_n^{\text{perm}}}\}$ describes realizations of a homogeneous Poisson point process with n ordered points over the duration $[0, 1]$ (compare also with left lower quadrant of Figure 1).

B. Rate-Distortion Problem on the Permutation Group

When considering a rate-distortion problem for a certain source, sometimes there exists a “natural choice” of a distortion measure that “preserves” the geometry of the source. The most typical example is the ℓ_2 -distortion measure for the Gaussian source, where the ℓ_2 -distortion ball has the same fundamental shape¹ as the source ball. Based on such a

¹Recall that for large n , with very high probability the source output sequences lie in a thin sphere. Thus when referring to the “source shape” we actually consider the geometry of the typical sequences.

geometric picture one can then use the idea of sphere- or ball-covering to derive (the converse to) the rate-distortion theorem (see, e.g., [1]).

In the following we will show how a natural choice of distortion measure can be found for the permutation group G_n^{perm} (n -cube) and for its subgroup $\{\mathbf{e}_{G_n^{\text{perm}}}\}$ (n -simplex) and how they lead to two well-known rate-distortion problems of the homogeneous Poisson process, namely the point-covering distortion problem [2], [3] and the canonical queueing distortion problem [4]. We will refer to these two cases as ℓ_∞ -ball covering for the homogeneous Poisson process.²

In this work, we distinguish the *source space* \mathcal{X} , which is the set of all possible source output sequences of a given length n , and the *source set* \mathcal{T} , which describes the geometry of the length- n typical sequences. The *codeword space* $\hat{\mathcal{X}}$ is the set of possible codeword sequences of length n .

In this section, (the closure of) our source set \mathcal{T} is the n -dimensional hypercube \square^n or the n -simplex \mathcal{S}_{σ_1} . Note that for the two rate-distortion problems on the permutation group we have $\mathcal{X} = \mathcal{T}$.

Then, for a given codeword $\mathbf{x}^* \in \text{cl}(\hat{\mathcal{X}})$ and for an allowed distortion D (normalized by the total duration T , yielding $0 < D \leq 1$), we define the *distortion set* $\mathcal{E}_{\mathbf{x}^*}(D)$ as follows:

$$\mathcal{E}_{\mathbf{x}^*}(D) \triangleq \lim_{\hat{\mathbf{x}} \rightarrow \mathbf{x}^*} \{\mathbf{t} \in \mathcal{X} : d(\mathbf{t}, \hat{\mathbf{x}}) \leq D\}, \quad (11)$$

where a limit is required here because due to the strict inequalities in (7) the codeword space $\hat{\mathcal{X}}$ is not closed.

Next we make more precise what we mean by “a natural choice” of distortion measure.

Definition 5 (Natural Distortion Measure): A distortion measure $d(\cdot, \cdot)$ is said to be *natural* if the distortion set defined in (11) preserves the geometry of the corresponding source set \mathcal{T} in the sense that there exists a unique $\mathbf{x}^* \in \text{cl}(\hat{\mathcal{X}})$ such that

$$\text{cl}(\mathcal{E}_{\mathbf{x}^*}(1)) = \text{cl}(\text{conv}(\{\mathbf{0}\} \cup \mathcal{T})). \quad (12)$$

Note that due to the normalization of timings we can set $T = 1$ without loss of generality.

1) Point-Covering Distortion: A rate-distortion codeword for the homogeneous Poisson process for the point-covering distortion is a $\{0, 1\}$ -valued signal $\hat{\mathbf{x}}$ on the interval $[0, 1]$ (see [2], [3]). The signal $\hat{\mathbf{x}}$ partitions $[0, 1]$ into a 1-valued, Lebesgue-measurable set $\mathcal{A}_{\hat{\mathbf{x}}}$ and a 0-valued set $\mathcal{A}_{\hat{\mathbf{x}}}^c$. The *point-covering distortion measure* $d_{\text{pc}}(\mathbf{t}, \hat{\mathbf{x}})$ between a point process realization \mathbf{t} and a codeword $\hat{\mathbf{x}}$ is the Lebesgue measure of $\mathcal{A}_{\hat{\mathbf{x}}}$, if $\mathcal{A}_{\hat{\mathbf{x}}}$ covers \mathbf{t} ; and is infinite otherwise:

$$d_{\text{pc}}(\mathbf{t}, \hat{\mathbf{x}}) = \begin{cases} \int_0^T \hat{x}(s) ds & \text{if } \int_0^T \hat{x}(s) \sum_{i=1}^n \delta(t_i - s) ds = n, \\ \infty & \text{otherwise} \end{cases} \quad (13)$$

(see also “dist.” in left upper quadrant of Figure 1).

²Other rate-distortion problems for the Poisson process that we do not consider here can be found, e.g., in [5]–[8].

Let \mathbf{t} be a Poisson point pattern of n points. Each codeword $\hat{\mathbf{x}}$ with $\mathcal{A}_{\hat{\mathbf{x}}}$ of Lebesgue measure D ($0 < D \leq 1$) gives the distortion set $\mathcal{E}_{\hat{\mathbf{x}}}(D) \subset \mathbb{R}^n$:

$$\begin{aligned} \mathcal{E}_{\hat{\mathbf{x}}}(D) &= \{\mathbf{t} \in \square^n : d_{\text{pc}}(\mathbf{t}, \hat{\mathbf{x}}) = D\} \\ &= \{\mathbf{t} \in \square^n : t_i \in \mathcal{A}_{\hat{\mathbf{x}}}, \forall i \in [n]\} \end{aligned} \quad (14)$$

for $\hat{\mathbf{x}}$ such that $\text{vol}_1(\mathcal{A}_{\hat{\mathbf{x}}}) = D$. Clearly, $\text{vol}_n(\mathcal{E}_{\hat{\mathbf{x}}}(D)) = D^n$. The minimal number of distortion sets needed to cover the n -cube is thus

$$\frac{\text{vol}_n(\square^n)}{\text{vol}_n(\mathcal{E}_{\hat{\mathbf{x}}}(D))} = \frac{1}{D^n}. \quad (15)$$

This gives the minimal rate of $\log(1/D)$ bits per point (i.e., per dimension).

When again including the duration T , we note that for a homogeneous Poisson process of rate λ , the expected number of points $\mathbb{E}[n] = \lambda T$. The resulting minimal average number of bits per unit time is therefore lower-bounded by $\frac{\mathbb{E}[n]}{T} \log(1/D) = \lambda \log(1/D)$, which is indeed the rate-distortion function for the Poisson process with the point-covering distortion measure [2], [3].

We have shown how the rate-distortion problem of the homogeneous Poisson process with point-covering distortion can be understood as covering an n -cube with the distortion set in (14). This cube covering perspective is similar to the converse proof given in [3], [9]. The resulting rate-distortion function shows this simple form in principle because the distortion set in (14) is matched to the source set, i.e., in other words, the point-covering distortion is a natural distortion measure for $\mathcal{T} = \square^n$ in that it satisfies the condition given in Definition 5. The geometry of the distortion set in \mathbb{R}^n matches that of the permutation group $\mathbb{G}_n^{\text{perm}}$.

2) *Canonical Queueing Distortion:* In this section, we describe point process realizations of n points over $[0, T]$ as a tuple \mathbf{t} of timings such that $t_1 < t_2 < \dots < t_n$. Thus, when the timings are normalized by the duration T , we have $\mathbf{t} \in \mathcal{S}_{\sigma_1}$, and $\mathcal{T} = \mathcal{S}_{\sigma_1}$ is the source set (see also left lower quadrant of Figure 1).

For the queueing rate-distortion problem, a codeword $\hat{\mathbf{x}}$ is also a point process realization over $[0, T]$ with timing description in the same ordered fashion $\hat{x}_1 < \hat{x}_2 < \hat{x}_3 < \dots$.

Let $N_{\mathbf{P}}(\cdot)$ be the counting function on the point process \mathbf{P} . The queueing distortion measure is defined as [4]

$$d_q(\mathbf{t}, \hat{\mathbf{x}}) \triangleq \begin{cases} \frac{1}{T} \sum_{i=1}^{N_{\hat{\mathbf{x}}}(T)} (t_i - \max\{t_{i-1}, \hat{x}_i\}) & \text{if } N_{\hat{\mathbf{x}}}(T) = N_{\mathbf{t}}(T) \\ & \text{and } N_{\hat{\mathbf{x}}}(s) \geq N_{\mathbf{t}}(s) \forall s \in [0, T], \\ \infty & \text{otherwise.} \end{cases} \quad (16)$$

Without loss of generality, we continue this section by considering normalized timings for point process realizations (timings normalized by the duration T). The conditions under which $d_q(\mathbf{t}, \hat{\mathbf{x}})$ is finite can be rewritten as follows.

Proposition 6: For two (normalized) point process realizations $\mathbf{t}, \hat{\mathbf{x}} \in \mathcal{S}_{\sigma_1}$ with $N_{\hat{\mathbf{x}}}(1) = N_{\mathbf{t}}(1) = n$, the following equivalence holds:

$$N_{\hat{\mathbf{x}}}(s) \geq N_{\mathbf{t}}(s) \forall s \in [0, 1] \iff t_i \geq \hat{x}_i \forall i \in [n]. \quad (17)$$

Following similar arguments as in Section II-B1, we will proceed to show next how the rate distortion problem of the homogeneous Poisson process with a canonical queueing distortion measure can be understood as covering the subgroup³ $\{\mathbf{e}_{\mathbb{G}_n^{\text{perm}}}\}$ (a simplex) with a natural distortion set.

Recall from (11) that the distortion set under distortion D for a given $\mathbf{x}^* \in \text{cl}(\mathcal{X})$ is

$$\mathcal{E}_{\mathbf{x}^*}(D) \triangleq \lim_{\hat{\mathbf{x}} \rightarrow \mathbf{x}^*} \{\mathbf{t} \in \mathcal{S}_{\sigma_1} : d_q(\mathbf{t}, \hat{\mathbf{x}}) \leq D\}. \quad (18)$$

In general, the shape of this set is quite complicated because of the maximum function contained in the queueing distortion measure (16). To help the reader with the following observations, in Appendix A we present a more detailed study of this exact shape for the case of $n = 2$.

We observe that for $\mathbf{x}^* = \mathbf{0}$, we have $\mathcal{E}_{\mathbf{0}}(1) = \mathcal{S}_{\sigma_1}$ and therefore, according to Definition 5, the queueing distortion $d_q(\cdot, \cdot)$ is a natural distortion measure for the source set $\mathcal{T} = \mathcal{S}_{\sigma_1}$. Note that for $\mathbf{x}^* = \mathbf{0}$ and arbitrary $0 < D \leq 1$

$$\mathcal{E}_{\mathbf{0}}(D) = D\mathcal{S}_{\sigma_1}, \quad (19)$$

where $D\mathcal{S}_{\sigma_1}$ denotes \mathcal{S}_{σ_1} scaled linearly by D . Thus, in this case the distortion set is a scaled version of the source set.

On the other hand, for a codeword $\hat{\mathbf{x}} \neq \mathbf{0}$, the distortion set $\mathcal{E}_{\hat{\mathbf{x}}}(D)$ is not necessarily a simplex (see Example 2 and Figure 4b in Appendix A). Nevertheless, $\hat{\mathbf{x}}$ can always be chosen such that the volume of the distortion set is preserved in the sense that for $N_{\hat{\mathbf{x}}}(1) = N_{\mathbf{t}}(1) = n$,

$$\sup_{\hat{\mathbf{x}} \in \mathcal{S}_{\sigma_1}} \text{vol}_n(\mathcal{E}_{\hat{\mathbf{x}}}(D)) = \text{vol}_n(D\mathcal{S}_{\sigma_1}). \quad (20)$$

Therefore, the minimal number of distortion sets needed to cover the source n -simplex $\mathcal{T} = \mathcal{S}_{\sigma_1}$ is

$$\frac{\text{vol}_n(\mathcal{S}_{\sigma_1})}{\sup_{\hat{\mathbf{x}} \in \mathcal{S}_{\sigma_1}} \text{vol}_n(\mathcal{E}_{\hat{\mathbf{x}}}(D))} = \frac{\text{vol}_n(\mathcal{S}_{\sigma_1})}{\text{vol}_n(D\mathcal{S}_{\sigma_1})} = \left(\frac{1}{D}\right)^n. \quad (21)$$

This gives again $\log(1/D)$ bits per point (per dimension) and, following the same arguments as in Section II-B1, we obtain the minimal number of bits per unit time $\lambda \log(1/D)$. This corresponds to the rate-distortion function for the Poisson process with the canonical queueing distortion measure [4].

Remark 7: Note that when D is very small, for all $\mathbf{t} \in \mathcal{E}_{\hat{\mathbf{x}}}(D)$ the following holds:

$$\hat{x}_{i+1} > t_i \geq \hat{x}_i \forall i \in [n-1], \text{ and } 1 > t_n \geq \hat{x}_n, \quad (22)$$

and thus

$$d_q(\mathbf{t}, \hat{\mathbf{x}}) = \sum_{i=1}^{N_{\mathbf{t}}(1)} (t_i - \hat{x}_i). \quad (23)$$

Therefore and because of Proposition 6, we see that in this situation

$$\mathcal{E}_{\hat{\mathbf{x}}}(D) = \hat{\mathbf{x}} + \text{cl}(D\delta), \quad (24)$$

where $D\delta$ is a scaled version of the simplex

$$\delta \triangleq \left\{ \Delta \mathbf{t} \in \mathbb{R}^n : \sum_{i=1}^n \Delta t_i < 1, \Delta t_i > 0 \forall i \in [n] \right\}. \quad (25)$$

³We loosely say ‘‘covering a group’’, but actually it means covering the union of all sets that constitutes the group.

Thus, here the distortion set is shaped like a scaled version of the simplex δ . Note that albeit the simplex δ is not similar to the source set \mathcal{S}_{σ_1} for $n \geq 3$, they have the same n -dimensional volume. For an exposition on $n = 2$, see Example 1 in Appendix A, where the distortion set $\mathcal{E}_{\hat{\mathbf{x}}}(D)$ is represented by the red triangle in Figure 3.

III. RATE DISTORTION AND ℓ_1 -SPHERE COVERING FOR THE HOMOGENEOUS POISSON PROCESS

We have shown in Sections II-B1 and II-B2 that with the timing description of point-process realizations, two known rate-distortion problems for the homogeneous Poisson point process (namely with point-covering distortion and with the canonical queuing distortion) can be understood geometrically as minimal covering problems for the permutation group (cube) and its subgroup (simplex), respectively. It is natural at this point to ask whether other interesting rate-distortion problems arise by considering minimal coverings of another group and its subgroup.

To that goal, recall that the inter-event interval τ of a homogeneous Poisson point process is exponentially distributed:

$$\tau \sim \lambda e^{-\lambda\tau} \mathbf{1}\{\tau \geq 0\}. \quad (26)$$

We now make the following two motivating observations:

- 1) If a vector of inter-event intervals describes the realization of a Poisson point process according to (26), then it lies close to a simplex $\Delta^{n-1}(n/\lambda)$ in \mathbb{R}^n if n is large.
- 2) The number of symmetries of $\Delta^{n-1}(n/\lambda)$ in \mathbb{R}^n can be increased by reflections, through which the simplex becomes the ℓ_1 -sphere $\mathcal{O}_1^{n-1}(n/\lambda)$.

Based on these two observations and analogously to what we have shown for the permutation group in Section II, in the rest of this section we study the reflection group and its associated rate distortion problems, namely the *Laplacian- ℓ_1* and the *exponential onesided- ℓ_1* rate-distortion problems.

A. The Regular Hyperoctahedron and the Reflection Group

We proceed to show that the ℓ_1 -sphere $\mathcal{O}_1^{n-1}(1)$, i.e., the boundary of a regular hyperoctahedron in \mathbb{R}^n , is isomorphic to the reflection group H_n .

We define for any $\mathbf{r} = (r_1, \dots, r_n)$ and $\mathcal{A} \subseteq \mathbb{R}^n$,

$$\mathbf{r} \odot \mathcal{A} \triangleq \{\mathbf{x} \in \mathbb{R}^n : x_i = r_i a_i \forall i \in [n] \text{ and } \mathbf{a} \in \mathcal{A}\}. \quad (27)$$

Definition 8: We define

$$G_n^{\text{refl}} \triangleq \{\mathbf{h} \odot \Delta^{n-1}(1) : \mathbf{h} \in H_n\} \quad (28)$$

with group operation “ $*$ ” given as follows:

$$\begin{aligned} & (\mathbf{h} \odot \Delta^{n-1}(1)) * (\mathbf{h}' \odot \Delta^{n-1}(1)) \\ & \triangleq (\mathbf{h} \cdot \mathbf{h}') \odot \Delta^{n-1}(1), \quad \mathbf{h}, \mathbf{h}' \in H_n. \end{aligned} \quad (29)$$

We note that, by definition, G_n^{refl} is isomorphic to H_n .

Proposition 9: The mapping

$$\varphi_r : H_n \rightarrow G_n^{\text{refl}}, \quad \mathbf{h} \mapsto \mathbf{h} \odot \Delta^{n-1}(1) \quad (30)$$

is an isomorphism.

Remark 10: Because of this isomorphism we henceforth also refer to G_n^{refl} as the reflection group.

The identity element of G_n^{refl} is

$$e_{G_n^{\text{refl}}} = \varphi_r(e_{H_n}) = \Delta^{n-1}(1) \quad (31)$$

with e_{H_n} being the identity element of H_n .

We will show in the following section that the reflection group G_n^{refl} and its subgroup $\{e_{G_n^{\text{refl}}}\}$ with their respective natural distortion measures yield the *Laplacian- ℓ_1* and the *exponential onesided- ℓ_1* rate-distortion problem.

B. Rate-Distortion Problem on the Reflection Group

Similarly to the discussion for the permutation group in Section II-B, we now consider the rate-distortion and minimal covering problem on the reflection group and its subgroup: G_n^{refl} (ℓ_1 -sphere $\mathcal{O}_1^{n-1}(1)$) and $\{e_{G_n^{\text{refl}}}\}$ (simplex $\Delta^{n-1}(1)$).

Recall from Observation 1) at the start of this section that the inter-event interval realizations generated by (26) lie almost surely in the thin shell around $\Delta^{n-1}(n/\lambda)$ (for a sufficiently large number of intervals); compare also with the schematic in right lower quadrant in Figure 1. Furthermore, we implement Observation 2) by labeling each inter-event interval independently with -1 or 1 equiprobably. This labeling creates a new source τ_s of *signed* inter-event intervals that has a Laplacian distribution:

$$\tau_s \sim \frac{\lambda}{2} e^{-\lambda|\tau_s|}. \quad (32)$$

Its realizations of length- n sequences lie almost surely in the thin shell around the ℓ_1 -sphere $\mathcal{O}_1^{n-1}(n/\lambda)$ (compare also with the schematic in right upper quadrant in Figure 1). We use again the notions of the source set \mathcal{T} and natural distortion measure introduced in Section II-B, and we consider two source sets⁴ $\mathcal{T} = \mathcal{O}_1^{n-1}(n/\lambda)$ or $\mathcal{T} = \Delta^{n-1}(n/\lambda)$, with their respective natural distortion measures. We refer to these two cases as ℓ_1 -sphere covering.

Again, using the same ideas based on the geometric picture of source set and distortion set, one can derive the rate-distortion functions for these two rate-distortion problems, see for example [1]. In the following we will only briefly summarize the results and omit their geometric derivations.

1) *Laplacian- ℓ_1 Rate-Distortion Problem:* The *normalized ℓ_1 -distortion measure* is defined as

$$d_{\text{norm}}(\mathbf{x}, \hat{\mathbf{x}}) \triangleq \frac{\lambda}{n} \sum_{i=1}^n |x_i - \hat{x}_i|, \quad (33)$$

where λ is the parameter of the Laplacian source in (32). It is easy to verify that the normalized ℓ_1 -distortion measure is a natural distortion measure for $\mathcal{T} = \mathcal{O}_1^{n-1}(n/\lambda)$.

The following lemma follows directly from [10, Lemma 6].

Lemma 11: For a Laplacian source (32) and the normalized ℓ_1 -distortion measure (33), the rate distortion function is

$$R_{\text{Laplacian}}(D) = \log\left(\frac{1}{D}\right) \mathbf{1}\{0 < D \leq 1\}. \quad (34)$$

⁴Note that $\mathcal{X} \neq \mathcal{T}$ for the two rate-distortion problems on the reflection group. The source spaces for the Laplacian and exponential source are $\mathcal{X} = \{\mathbf{x} \in \mathbb{R}^n : x_i \neq 0 \forall i \in [n]\}$ and $\mathcal{X} = \{\mathbf{x} \in \mathbb{R}^n : x_i > 0 \forall i \in [n]\}$, respectively.

2) *Exponential Onesided- ℓ_1 Rate-Distortion Problem*: The normalized onesided ℓ_1 -distortion measure is defined as

$$d_1(\mathbf{x}, \hat{\mathbf{x}}) \triangleq \begin{cases} \frac{\lambda}{n} \sum_{i=1}^n |x_i - \hat{x}_i| & \text{if } x_i - \hat{x}_i \geq 0 \forall i \in [n], \\ \infty & \text{otherwise,} \end{cases} \quad (35)$$

where λ is the parameter of the exponential source in (26). Again, one can verify that $d_1(\cdot, \cdot)$ is a natural distortion measure for $\mathcal{T} = \Delta^{n-1}(n/\lambda)$.

The following lemma follows directly from [10, Lemma 2].

Lemma 12: For an exponential source (26) and the normalized onesided ℓ_1 -distortion measure (35), the rate-distortion function is

$$R_{\text{Exponential}}(D) = \log\left(\frac{1}{D}\right) \mathbf{1}\{0 < D \leq 1\}. \quad (36)$$

Note that when viewing n as the number of points in a point process realization, the rate-distortion functions in Lemmas 11 and 12 are the same function, measured in bits per symbol (per point). This gives $\log(1/D)$ bits per point just as the results in Sections II-B1 and II-B2. Therefore, when considering the rate-distortion problem under the inter-event interval description of a homogeneous Poisson process of rate λ , we see that we use $n \log(1/D)$ bits to describe a complete sequence of (random) duration $T_{\text{tot}}(n)$, and thus the number of bits per unit time, for large n , is

$$\lim_{n \rightarrow \infty} \frac{n \log\left(\frac{1}{D}\right)}{T_{\text{tot}}(n)} = \lim_{n \rightarrow \infty} \frac{\log\left(\frac{1}{D}\right)}{\frac{T_{\text{tot}}(n)}{n}} = \frac{\log\left(\frac{1}{D}\right)}{\frac{1}{\lambda}}, \quad (37)$$

and we obtain the minimal number of bits per unit time $\lambda \log(1/D)$.

It is not a coincidence that all four rate-distortion functions in Sections II-B1, II-B2, III-B1, III-B2 are the same. The reason is that they all have their own natural distortion sets matched to their source sets, i.e., they all satisfy the criterion given in Definition 5.

To this point, we have presented the rate-distortion problems of the Poisson process as ℓ_∞ -ball covering in Section II and ℓ_1 -sphere covering in Section III. One may wonder why it exactly is ℓ_∞ and ℓ_1 . We attempt to answer this question in the following section by exploring the *hyperoctahedral group*, which is the group of symmetries of the hypercube or the regular hyperoctahedron.

IV. THE HYPEROCTAHEDRAL GROUP AND HOW IT IS GENERATED FROM THE POISSON PROCESS

The *hyperoctahedral group*, denoted O_n , describes the symmetries of both an n -dimensional hypercube or an n -dimensional regular hyperoctahedron (see, e.g., [11]). In other words, the n -cube and the n -dimensional regular hyperoctahedron have the same group of symmetries and are both realizations of the group of symmetries O_n in \mathbb{R}^n .

This can be understood most easily when realizing that the regular hyperoctahedron and the hypercube are actually dual (polar) polytopes: replacing the vertices of one by $(n-1)$ -dimensional faces results in the other and vice-versa. This geometric duality means that we can inscribe one in the other in such a way that it becomes straightforward to see that the two share the same symmetries.

In the following we are going to show that the hyperoctahedral group can be understood as being “spanned” (by means of the semidirect product) by the reflection group G_n^{refl} and the permutation group G_n^{perm} (see Theorem 28 below). To that goal, we will in a first step derive the symmetries of a general polytope and describe them by means of a permutation subgroup over its vertices (Lemma 21). In a second step, we will then relate the group of symmetries of the regular hyperoctahedron and of the hypercube with the automorphism group of their respective graph (Theorems 26 and 27).

The ultimate goal of this section is to give a (partial) answer to our original question posed at the end of the previous section: Why exactly do ℓ_∞ (cube) and ℓ_1 (octahedron) show up? Recall that the Poisson process possesses two geometric descriptions (sets), namely the two simplices shown on the left and right column in Figure 1. For both descriptions we “added” some symmetrization, namely permutation (left column in Figure 1) or reflections (right column in Figure 1), to obtain the hypercube or the regular hyperoctahedron, respectively. The choice of these symmetrizations are not merely ad-hoc. To show this, we propose an iterative algorithm that iteratively “expands” the pair of source sets $\mathcal{T} = \mathcal{S}_{\sigma_1}$ and $\mathcal{T} = \Delta^{n-1}$ (and their respective symmetries) until their group of symmetries become isomorphic (at which point the algorithm ends). Applying this algorithm to the two simplices in the lower blue boxes in Figure 1, we arrive at a hypercube and a regular hyperoctahedron in the end. This is explained in more detail in Section IV-F and Figure 2.

A. Preliminaries

Definition 13: For $\varphi: X \rightarrow Y$, $x \mapsto \varphi(x)$ and $\mathcal{A} \subset X$, $\mathcal{B} \subset Y$, we say “ $\varphi(\mathcal{A}) = \mathcal{B}$ ” to mean “ $\varphi(x) \in \mathcal{B}$ if, and only if, $x \in \mathcal{A}$.”

Definition 14: An *isometry* of a metric space (X, d) is a surjective function

$$\varphi: X \rightarrow X, \quad x \mapsto \varphi(x) \quad (38)$$

such that

$$d(x, x') = d(\varphi(x), \varphi(x')), \quad \forall x, x' \in X. \quad (39)$$

The set⁵ of all isometries of a metric space X is denoted by $\text{Isom}(X)$.

Thus, an isometry is a mapping that preserves distances. Typical examples are rotations, reflections, or translations in the Euclidean space.

These isometries are now the basis for capturing the concept of *symmetries* of an object.

Definition 15 (The Group of Symmetries of a Set): For any $\mathcal{A} \subset E_n$, the *group of symmetries* of \mathcal{A} , denoted $\text{Sym}_{E_n}(\mathcal{A})$, is defined as

$$\text{Sym}_{E_n}(\mathcal{A}) \triangleq \{\varphi \in \text{Isom}(E_n) : \varphi(\mathcal{A}) = \mathcal{A}\}, \quad (40)$$

where the group operation is function composition.

So, any symmetry of some set is an isometry that maps the set back to itself.

⁵Note that $\text{Isom}(X)$ can be seen as a group where function composition is its group operation.

We also use the following standard group-theoretic definitions for a *group action on a set* and the *semidirect product*, see for example [12] as a reference.

Definition 16 (Group Action on a Set): The group G acts on a set \mathcal{X} if there is a function

$$f: G \times \mathcal{X} \rightarrow \mathcal{X}, (g, x) \mapsto gx \quad (41)$$

satisfying the following conditions:⁶

- $ex = x, \forall x \in \mathcal{X}$;
- $g_1(g_2x) = (g_1 \cdot g_2)x, \forall g_1, g_2 \in G, x \in \mathcal{X}$.

Here $e \in G$ is the identity element and “ \cdot ” is the group operation of G . We say that G acts on \mathcal{X} with (left) action⁷ f .

Definition 17 (Internal Semidirect Product): Let H_1 and H_2 be subgroups of G equipped with the group operation “ \cdot ” and with the identity element e_G . We say that G is the *internal semidirect product* of H_1 by H_2 , denoted $G = H_1 \rtimes H_2$, if

- H_1 is a normal subgroup⁸ of G , i.e., $g \cdot H_1 = H_1 \cdot g$ for all $g \in G$;
- $H_1 \cap H_2 = \{e_G\}$;
- $G = H_1 \cdot H_2$.

Finally, we are going to need *affine maps*:

Definition 18: Let V, W be real normed linear spaces. We say a map $\alpha: V \rightarrow W, v \mapsto \alpha(v)$ is *affine* if

$$\alpha(sv + (1-s)v') = s\alpha(v) + (1-s)\alpha(v'), \quad \forall v, v' \in V, s \in [0, 1]. \quad (42)$$

B. Polytopes and Group of Symmetries of Polytopes

Definition 19: A *polytope* \mathcal{P} is defined as the convex hull of a finite, nonempty set of points in \mathbb{R}^n , for some $n \geq 2$. The *dimension* of \mathcal{P} , denoted $\dim \mathcal{P}$, is defined as the dimension of the smallest linear subspace containing \mathcal{P} . We call \mathcal{P} a *k-polytope* when $\dim \mathcal{P} = k$.

Definition 20 (Extreme Points and Vertices of a Polytope): For a compact convex set $\mathcal{S} \subset \mathbb{R}^n$, we define $\mathbf{x} \in \mathcal{S}$ to be an *extreme point* if, and only if, $\mathcal{S} \setminus \{\mathbf{x}\}$ is also convex. The set of all extreme points of \mathcal{S} is denoted $\text{Extr}(\mathcal{S})$. When \mathcal{S} is a polytope, $\text{Extr}(\mathcal{S})$ is the set of vertices of the polytope. We denote the set of vertices of a polytope \mathcal{P} as $\mathcal{V}(\mathcal{P})$.

So, let \mathcal{P} be an n -polytope with its set of vertices

$$\mathcal{V}(\mathcal{P}) = \{\mathbf{x}_1, \mathbf{x}_2, \dots, \mathbf{x}_m\}, \quad (43)$$

where $\mathbf{x}_i \in \mathbb{R}^n, \forall i \in [m]$, and without loss of generality assume that

$$\frac{1}{m} \sum_{i \in [m]} \mathbf{x}_i = \mathbf{0}. \quad (44)$$

Let the permutation group S_m act on $\mathcal{V}(\mathcal{P})$ with action

$$g\mathbf{x}_i \triangleq \mathbf{x}_{gi}, \quad \forall g \in S_m \quad (45)$$

⁶Note that in this definition and for the rest of the article, we use the juxtaposition notation introduced in (41) for (left) group actions.

⁷Note that when we use the term “a group acts on a set”, we always refer to the *left* group action if not otherwise specified.

⁸Note that we make no assumption regarding G being Abelian.

(i.e., the vertices of \mathcal{P} are permuted), and define the subgroup $G_{\mathcal{V}(\mathcal{P})}$ of S_m as

$$G_{\mathcal{V}(\mathcal{P})} \triangleq \{g \in S_m : \|\mathbf{x}_i - \mathbf{x}_j\|_2 = \|g\mathbf{x}_i - g\mathbf{x}_j\|_2, \quad \forall \mathbf{x}_i, \mathbf{x}_j \in \mathcal{V}(\mathcal{P})\}, \quad (46)$$

i.e., $G_{\mathcal{V}(\mathcal{P})}$ contains all those permutations of the vertices of \mathcal{P} that preserves the pairwise ℓ_2 -distances between the vertices.

We will show next that $G_{\mathcal{V}(\mathcal{P})}$, which is defined using merely the vertices of the polytope, describes the symmetries of this (full-dimensional) n -polytope \mathcal{P} in \mathbb{R}^n , i.e., $G_{\mathcal{V}(\mathcal{P})}$ is isomorphic to the group of symmetries of \mathcal{P} .

Lemma 21 (Group of Symmetries of a Polytope): Consider the n -polytope \mathcal{P} and its group $G_{\mathcal{V}(\mathcal{P})}$ as defined above in (43)–(46). Then for any $g \in G_{\mathcal{V}(\mathcal{P})}$, there exists a unique affine map

$$\alpha_g: \mathbb{R}^n \rightarrow \mathbb{R}^n, \mathbf{x} \mapsto \alpha_g(\mathbf{x}) \quad (47)$$

satisfying

$$\alpha_g(\mathbf{x}_i) = g\mathbf{x}_i, \quad \forall \mathbf{x}_i \in \mathcal{V}(\mathcal{P}). \quad (48)$$

Moreover,

$$\text{Sym}_{E_n}(\mathcal{P}) = \{\alpha_g : g \in G_{\mathcal{V}(\mathcal{P})}\}, \quad (49)$$

and

$$\text{Sym}_{E_n}(\mathcal{P}) \cong G_{\mathcal{V}(\mathcal{P})}. \quad (50)$$

Proof: See Appendix B. ■

C. Graph of Polytopes and Automorphism Group of a Graph

Definition 22 (Basic Graph Definitions, see, e.g., [13]): Let $V \neq \emptyset$ be a nonempty set and denote the set of all k -element subsets of V by $[V]^k$. An *undirected graph* $\Gamma = (V, E)$ is a pair of sets where $E \subseteq [V]^2$. Here, V is called the *vertex set* and E is called the *edge set* of the graph. We say $v_1, v_2 \in V$ are *adjacent (vertices)* if $\{v_1, v_2\} \in E$.

Definition 23 (The Graph of a Polytope): The *graph of a polytope* \mathcal{P} , denoted $\Gamma_{\mathcal{P}}$, is an undirected graph formed by the vertices and the 1-dimensional faces (edges) of the polytope.

Definition 24 (Graph Isomorphism): Let $V, V' \neq \emptyset$. Two graphs $\Gamma = (V, E), \Gamma' = (V', E')$ are *isomorphic* if there exists a bijective function $\varphi: V \rightarrow V'$ such that $\{\varphi(v_1), \varphi(v_2)\} \in E'$ if, and only if, $\{v_1, v_2\} \in E$. We call φ a *graph isomorphism* from Γ to Γ' .

Definition 25 (Graph Automorphism): An *automorphism* of a graph $\Gamma = (V, E)$ is a graph isomorphism from Γ to itself. It thus follows that an automorphism is a permutation of the vertex set V that preserves both the *adjacencies* and the *nonadjacencies* of the graph Γ .

The collection of all automorphisms of a graph Γ is denoted $\text{Aut}(\Gamma)$, the *automorphism group* of Γ equipped with composition as group operation.

D. Auxiliary Theorems

We next show that, for both the hypercube and the regular hyperoctahedron, the group of symmetries and the automorphism group of its graph are isomorphic. Note that this is nontrivial. The crucial point is to realize that a graph of a polytope ignores distances, but only describes adjacencies and nonadjacencies. So, as a simple example, consider in \mathbb{R}^2 a square and a rectangle: both have the same graph, but obviously their group of symmetries are not identical.

We start with the regular hyperoctahedron, which allows for a simpler proof because the distance between any two vertices can only take one of two possible values.

Theorem 26: The group of symmetries of a regular hyperoctahedron is isomorphic to the automorphism group of its graph:

$$\text{Sym}_{E_n}(\diamond^n) \cong \text{Aut}(\Gamma_{\diamond^n}). \quad (51)$$

Proof: Let $\Gamma_{\diamond^n} = (V, E)$ be the graph of \diamond^n where $V = \mathcal{V}(\diamond^n)$ and therefore $|V| = 2n$. For any $g \in S_{2n}$, let $\varphi_g: V \rightarrow V$ be a graph isomorphism from (V, E) to (V, E') where $\varphi_g(\mathbf{v}) \triangleq g\mathbf{v}$, $\mathbf{v} \in V$. Then using Definition 25, $\varphi_g \in \text{Aut}(\Gamma_{\diamond^n})$ if, and only if, $E = E'$, which is equivalent to each of the following conditions:

- 1) Adjacency condition: For any $\mathbf{v}, \mathbf{v}' \in V$,

$$\{\mathbf{v}, \mathbf{v}'\} \in E \iff \{g\mathbf{v}, g\mathbf{v}'\} \in E. \quad (52)$$

- 2) Nonadjacency condition: For any $\mathbf{v}, \mathbf{v}' \in V$,

$$\{\mathbf{v}, \mathbf{v}'\} \in [V]^2 \setminus E \iff \{g\mathbf{v}, g\mathbf{v}'\} \in [V]^2 \setminus E. \quad (53)$$

Using the equivalence of conditions 1) and 2) above we can write the automorphism group as:

$$\begin{aligned} \text{Aut}(\Gamma_{\diamond^n}) &\cong \{g \in S_{2n} : \text{condition 1) holds}\} \\ &= \{g \in S_{2n} : \text{condition 1) and 2) hold}\} \end{aligned} \quad (54)$$

$$= \{g \in S_{2n} : \|\mathbf{v} - \mathbf{v}'\|_2 = \|g\mathbf{v} - g\mathbf{v}'\|_2, \forall \mathbf{v}, \mathbf{v}' \in \mathcal{V}(\diamond^n)\} \quad (56)$$

$$= G_{\mathcal{V}(\diamond^n)}, \quad (57)$$

where (56) holds because for any $\mathbf{v}, \mathbf{v}' \in V$

- $\{\mathbf{v}, \mathbf{v}'\} \in E \iff \|\mathbf{v} - \mathbf{v}'\|_2 = \sqrt{2}$, and
- $\{\mathbf{v}, \mathbf{v}'\} \in [V]^2 \setminus E \iff \|\mathbf{v} - \mathbf{v}'\|_2 = 2$.

Furthermore, applying Lemma 21 we have $\text{Sym}_{E_n}(\diamond^n) \cong G_{\mathcal{V}(\diamond^n)}$, and therefore $\text{Sym}_{E_n}(\diamond^n) \cong G_{\mathcal{V}(\diamond^n)} \cong \text{Aut}(\Gamma_{\diamond^n})$. This concludes the proof. ■

For a hypercube, vertices can be at various different distances to each other, depending on their relative position to each other. The proof of the isomorphism between the group of symmetries and the automorphism group is thus a bit more involved and moved to the appendix.

Theorem 27: The group of symmetries of a hypercube is isomorphic to the automorphism group of its graph:

$$\text{Sym}_{E_n}(\square^n) \cong \text{Aut}(\Gamma_{\square^n}). \quad (58)$$

Proof: See Appendix C. ■

E. The Hyperoctahedral Group and its Connection to the Permutation and Reflection Group

As already mentioned, the hyperoctahedral group O_n describes the symmetries of an n -dimensional hypercube or of an n -dimensional regular hyperoctahedron (cross-polytope).

The order $|O_n|$ of the hyperoctahedral group O_n is

$$|O_n| = 2^n n!. \quad (59)$$

For example in three dimensions, $|O_3| = 8 \cdot 6 = 48$. Note that O_3 can also be understood as a composition of (rigid-body) rotation and mirroring, which gives $|O_3| = 2 \cdot 24 = 48$.

As we have seen above, the group of symmetries of a hypercube or a regular hyperoctahedron is isomorphic to the automorphism group of the corresponding graph. Thus, it is possible to define the hyperoctahedral group as the automorphism group of the graph of the hypercube [14, Lecture 3].

So, let $Z_2 \triangleq \{0, 1\}$ be a group equipped with modulo-2 addition, and let Z_2^n be its n -fold direct product. It is known that $\text{Aut}(\Gamma_{\square^n})$ is isomorphic to the internal semidirect product of Z_2^n by the permutation group S_n [15], [14, Lecture 3]:

$$\text{Aut}(\Gamma_{\square^n}) \cong Z_2^n \rtimes S_n. \quad (60)$$

Clearly, $Z_2^n \cong H_n$. And since by Propositions 3 and 9 we have $S_n \cong G_n^{\text{perm}}$ and $H_n \cong G_n^{\text{refl}}$, we obtain the following result.

Theorem 28:

$$O_n \cong G_n^{\text{refl}} \rtimes G_n^{\text{perm}}. \quad (61)$$

By the third condition in Definition 17 for the internal semidirect product, we can understand Theorem 28 intuitively as the construction of O_n by two of its subgroups: the reflection subgroup G_n^{refl} and the permutation subgroup G_n^{perm} .

Remark 29: Note that by Frucht's theorem [16], one can construct a graph whose automorphism group is isomorphic to O_n . Unfortunately, when following Frucht's construction, we do not obtain the graph of a hypercube or a hyperoctahedron. This is why we had to use Lemma 21 and the two Theorems 26 and 27 to formally establish the *hyperoctahedral* group as both the symmetries of a polytope and the automorphism group of the graph of the polytope.

F. From the Poisson Process to O_n : an Algorithm

We propose the following recursive algorithm. We are given two (source) sets $\mathcal{T}_1^{(a)}$ and $\mathcal{T}_1^{(b)}$ and their corresponding group of symmetries $G_1^{(a)}$ and $G_1^{(b)}$, and we choose some group action according to Definition 16.

We now start with the group $G_1^{(b)}$ acting on $\mathcal{T}_1^{(a)}$ (according to the chosen group action) to create an enlarged set $\mathcal{T}_2^{(a)}$. Let $G_2^{(a)}$ denote the group of symmetries of $\mathcal{T}_2^{(a)}$. In a next step we let the group $G_2^{(a)}$ act on $\mathcal{T}_1^{(b)}$, and we obtain an enlarged set $\mathcal{T}_2^{(b)}$ with its group of symmetries $G_2^{(b)}$.

We repeat this process until the group of symmetries of the two sets become isomorphic. The goal is to choose the group actions in such a way that in each step $G_i^{(j)}$ is isomorphic to a subgroup of $G_{i+1}^{(j)}$, $j \in \{a, b\}$.

Applied to our situation of a hypercube and a regular hyperoctahedron, we define the group action on \mathbb{R}^n , $G \times \mathbb{R}^n \rightarrow$

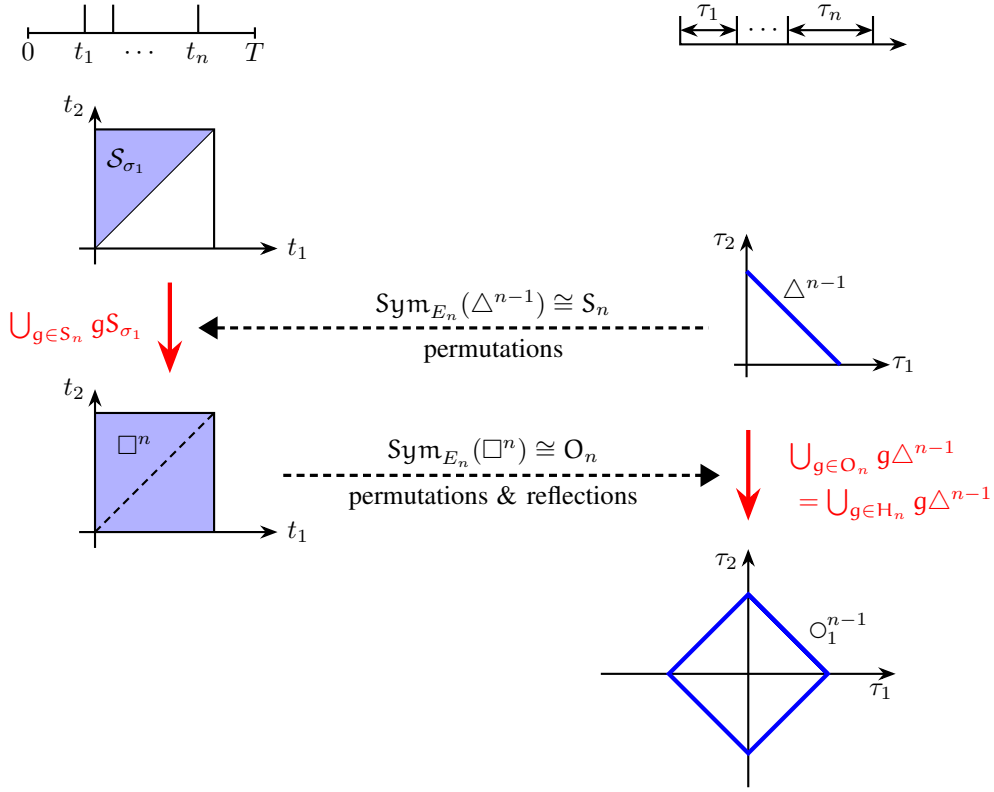


Fig. 2. Recursive algorithm to create the hyperoctahedral group from the symmetries in the two source sets of a Poisson process. The symmetries of the $(n-1)$ -simplex Δ^{n-1} are “added” to the n -simplex \mathcal{S}_{σ_1} , resulting in the cube \square^n . Then the symmetries of the cube \square^n are “added” to the $(n-1)$ -simplex Δ^{n-1} , resulting in the ℓ_1 -sphere \mathcal{O}_1^{n-1} . The group of symmetries of \square^n and \mathcal{O}_1^{n-1} are both isomorphic to O_n , and thus the algorithm stops.

\mathbb{R}^n , $(g, \mathbf{x}) \mapsto g\mathbf{x}$ for $G = S_n, H_n, O_n$, respectively, with matrix multiplications $\forall \mathbf{x} \in \mathbb{R}^n$ as follows.

(a) $G = S_n$; $\sigma \in S_n$ is a permutation:

$$\sigma \mathbf{x} \triangleq \mathbf{A}_\sigma \mathbf{x}, \quad (62)$$

where

$$[\mathbf{A}_\sigma]_{ij} = \mathbf{1}\{j = \sigma(i)\}; \quad (63)$$

(b) $G = H_n$; $h \in H_n$ is a reflection:

$$h \mathbf{x} \triangleq \mathbf{A}_h \mathbf{x}, \quad (64)$$

where

$$[\mathbf{A}_h]_{ij} = h(i) \mathbf{1}\{i = j\}; \quad (65)$$

(c) $G = O_n$; $o \in O_n$ is a signed permutation:

$$o \mathbf{x} \triangleq \mathbf{A}_o \mathbf{x}, \quad (66)$$

where

$$[\mathbf{A}_o]_{ij} = \text{sgn}(o(i)) \mathbf{1}\{j = |o(i)|\}. \quad (67)$$

Here, for $g \in G$, \mathbf{A}_g denotes a matrix in $\mathbb{R}^{n \times n}$; $[\cdot]_{ij}$ denotes the entry at the i th row and j th column of a matrix; and $|\cdot|$ denotes the absolute value.

We further define for $\mathcal{S} \subset \mathbb{R}^n$ and $g \in G$,

$$g\mathcal{S} \triangleq \{g\mathbf{x} : \mathbf{x} \in \mathcal{S}\}. \quad (68)$$

Using these groups actions (a)–(c) above and (68), we now apply the proposed algorithm to the source sets⁹ $\mathcal{T}_1^{(a)} = \mathcal{S}_{\sigma_1}$ and $\mathcal{T}_1^{(b)} = \Delta^{n-1}$. In this case the algorithm stops already after only two steps. The resulting sets are $\mathcal{T}_2^{(a)} = \square^n$ and $\mathcal{T}_2^{(b)} = \mathcal{O}_1^{n-1}$, both with group of symmetries isomorphic to O_n .

Figure 2 depicts a summary of this process.

This shows how our choice of permutation, reflection and hyperoctahedral group actually arise in a principled way by applying this algorithm to the source sets of the Poisson process.

Referring back to the graphical summary of Sections II and III in Figure 1, we conclude from this section that the hyperoctahedral group unifies the two columns of Figure 1, demonstrating the symmetries of a Poisson process.

V. DISCUSSION

A homogeneous Poisson process can be described by event (point) timings or inter-event (inter-point) intervals (compare with the left and right columns in Figure 1). Both descriptions give rise to a group theoretic view point (conditioned on a given number of points), namely the timing description corresponds to the *permutation group* and the interval description leads to the *reflection group*. These in combination with properly chosen distortion measures allow the corresponding

⁹Recall that, these two source sets arise from the timing and interval description of the Poisson process, respectively.

rate-distortion problem to be expressed as a ball- or sphere-covering problem.

Concretely, in Section II we considered the permutation group and its subgroup to describe the point-covering rate-distortion problem and the queueing rate-distortion problem, respectively, and showed them to correspond to ℓ_∞ -ball covering. In Section III we considered the reflection group and its subgroup to describe the exponential onesided ℓ_1 -rate-distortion problem and the Laplacian ℓ_1 -rate-distortion problem, respectively, and showed them to correspond to ℓ_1 -sphere covering.

We also defined the *natural distortion measure* which guarantees the distortion set around a codeword has a similar shape to the source set. And in Section IV, we presented the hyperoctahedral group which can be realized as a hypercube or a regular hyperoctahedron, and we showed that the permutation group and the reflection group give a construction of the hyperoctahedral group via the semidirect product. This demonstrates the connections between the hyperoctahedral group and the symmetries of a Poisson process.

We also would like to point out that the Poisson point process induces asymptotically a uniform distribution over each of the source-set simplices (see illustration in lower left and lower right blue boxes in Figure 1). This is one of the reasons why the ratio of volume of source set to volume of distortion set eventually leads to the required description rate. Although similar sphere-covering arguments apply even if we did not have a uniform distribution over the source set, the converse based on sphere covering with equally-sized distortion balls will not be tight anymore, as the compression could be improved by smaller distortion balls in areas of higher probability.

Our geometric approach also works in the case of an inhomogeneous Poisson process for the situation of point covering [3]. There we need to rescale time in the following way: for a fixed (infinitesimal small) interval $[t, t + dt]$, we define a rate $\tilde{\lambda} \triangleq \frac{\lambda(t) dt}{T}$ and assume a given distortion \tilde{D} . Then, the geometric arguments from Section II-B1 yield the lower bound $\lambda(t) dt \log(1/\tilde{D})$ to the minimum number of bits over the interval $[t, t + dt]$. Integrating all these lower bounds over t , where \tilde{D} is replaced by $D(t)$, and minimizing over the choice of $D(t)$ then yields the rate-distortion function as given in [3, Th. 2].

APPENDIX A

DISTORTION SETS FOR THE QUEUEING DISTORTION

In this section, we elaborate some arguments in Section II-B2 about the (shape of the) queueing distortion set, with two illustrative examples for $N_{\hat{\mathbf{x}}}(1) = N_{\mathbf{t}}(1) = 2$.

Recall that for normalized timings (all timings t_k normalized by duration T), $\{e_{G_n^{\text{perm}}}\}$ gives the source set \mathcal{T} for the canonical queueing distortion, i.e., $\mathcal{T} = S_{\sigma_1}$. For $n = 2$, the closure of \mathcal{T} is illustrated in Figure 3 as the 2-simplex with its set of vertices $\mathcal{T}^0 = \{(0, 0), (0, 1), (1, 1)\}$. Thus, for a given $\hat{\mathbf{x}}$, the subset $\mathcal{R}_{d_q < \infty}(\hat{\mathbf{x}}) \subseteq \mathcal{T}$ of points resulting in a finite queueing distortion $d_q(\mathbf{t}, \hat{\mathbf{x}}) < \infty$ can be written as follows:

$$\mathcal{R}_{d_q < \infty}(\hat{\mathbf{x}}) \triangleq \{\mathbf{t} \in \mathcal{T} : d_q(\mathbf{t}, \hat{\mathbf{x}}) < \infty\}$$

$$= \{\mathbf{t} \in \mathcal{T} : t_k \geq \hat{x}_k \forall k \in [n]\} \quad (69)$$

(compare with Proposition 6).

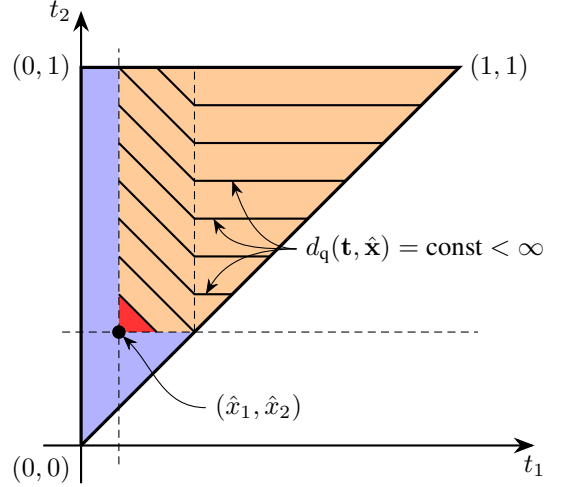


Fig. 3. The 2-simplex illustrated here represents the source set $\mathcal{T} = S_{\sigma_1}$ for $n = 2$. It is partitioned into four regions by a given $\hat{\mathbf{x}} = (\hat{x}_1, \hat{x}_2)$. The orange partition $\mathcal{R}_{d_q < \infty}(\hat{\mathbf{x}})$ consists of all realizations $\mathbf{t} = (t_1, t_2)$ where the queueing distortion $d_q(\mathbf{t}, \hat{\mathbf{x}})$ is finite. On the other hand, for all \mathbf{t} in the blue partitions, $d_q(\mathbf{t}, \hat{\mathbf{x}}) = \infty$. The black contour lines depict “isolines” of constant distortion. The red triangle depicts the distortion set according to a situation described in Example 1.

Figure 3 illustrates $\mathcal{R}_{d_q < \infty}(\hat{\mathbf{x}})$ in orange for $n = 2$. With the geometric picture of Figure 3, we can now illustrate the distortion set for $\hat{\mathbf{x}} = (\hat{x}_1, \hat{x}_2)$ in \mathbb{R}^2 under two disjoint conditions, see Example 1 and 2.

Example 1: Consider $\hat{\mathbf{x}} = (\hat{x}_1, \hat{x}_2)$ where $0 < \hat{x}_1 < \hat{x}_2 < 1$. Then for $0 < D \leq \hat{x}_2 - \hat{x}_1$, the distortion set is

$$\mathcal{E}_{\hat{\mathbf{x}}}(D) = \left\{ \mathbf{t} \in \mathbb{R}^2 : \sum_{i=1}^2 (t_i - \hat{x}_i) \leq D, \right. \\ \left. t_k \geq \hat{x}_k \forall k \in [2], t_1 \neq t_2 \right\}. \quad (70)$$

Figure 3 shows an exemplary such set in red. We see that in this case the distortion set is $\hat{\mathbf{x}} + \text{cl}(D\delta) \setminus \{(\hat{x}_2, \hat{x}_2)\}$ (compare also with (24)).

Example 2: Consider $\hat{\mathbf{x}} = (\hat{x}_1, \hat{x}_2)$ where $0 < \hat{x}_1 < \hat{x}_2 < 1$. Then for $\hat{x}_2 - \hat{x}_1 < D \leq 1$, to obtain the distortion set we partition $\mathcal{R}_{d_q < \infty}(\hat{\mathbf{x}})$ (see (69)) along

$$\mathcal{L}_2 \triangleq \{\mathbf{t} \in \mathbb{R}^2 : t_1 = \hat{x}_2\} \quad (71)$$

into \mathcal{R}_1 and \mathcal{R}_2 as follows:

$$\mathcal{R}_1 \triangleq \mathcal{R}_{d_q < \infty}(\hat{\mathbf{x}}) \cap \mathcal{L}_2^- \\ = \{(t_1, t_2) \in \mathcal{R}_{d_q < \infty}(\hat{\mathbf{x}}) : \hat{x}_1 \leq t_1 < \hat{x}_2 \leq t_2\}, \quad (72)$$

$$\mathcal{R}_2 \triangleq \mathcal{R}_{d_q < \infty}(\hat{\mathbf{x}}) \cap \mathcal{L}_2^{+,0} \\ = \{(t_1, t_2) \in \mathcal{R}_{d_q < \infty}(\hat{\mathbf{x}}) : \hat{x}_1 < \hat{x}_2 \leq t_1 < t_2\}, \quad (73)$$

where

$$\mathcal{L}_2^- \triangleq \{\mathbf{t} \in \mathbb{R}^2 : t_1 < \hat{x}_2\}, \quad (74)$$

$$\mathcal{L}_2^{+,0} \triangleq \{\mathbf{t} \in \mathbb{R}^2 : t_1 \geq \hat{x}_2\}. \quad (75)$$

In Figure 4a, \mathcal{R}_1 and \mathcal{R}_2 are represented by the light orange and dark orange regions, respectively. The types of point pattern corresponding to either \mathcal{R}_1 and \mathcal{R}_2 are illustrated as either the light or dark orange spike pattern in the middle of Figure 4.

The distortion measure given by (16) can now be rewritten depending on whether the realization $\mathbf{t} = (t_1, t_2)$ lies in \mathcal{R}_1 or \mathcal{R}_2 as follows:

$$d_q(\mathbf{t}, \hat{\mathbf{x}}) = \begin{cases} (t_1 - \hat{x}_1) + (t_2 - \hat{x}_2) & \mathbf{t} \in \mathcal{R}_1, \\ t_2 - \hat{x}_1 & \mathbf{t} \in \mathcal{R}_2. \end{cases} \quad (76)$$

Using (76), a contour line of constant distortion D is depicted in black in Figure 4a. The distortion set $\mathcal{E}_{\hat{\mathbf{x}}}(D)$ is thus as shown in Figure 4b in yellow. So clearly the shape is not a simplex. But since the volume of triangle 1 equals that of triangle 2 in Figure 4b, the volume of the distortion set $\mathcal{E}_{\hat{\mathbf{x}}}(D)$ equals the volume of the simplex $D\delta$. In other words, Example 2 gives a distortion set that is not similar (in shape) to the scaled source set DS_{σ_1} , yet preserves the volume of it.

APPENDIX B PROOF OF LEMMA 21

A. Preliminaries for the Proof

Theorem 30 (Mazur-Ulam Theorem (1932) [17], [18]): Any bijective isometry between real normed spaces X and Y , $\varphi: X \rightarrow Y$, is an affine map.

Applying this theorem to an isometry from E_n to E_n leads immediately to the following corollary.

Corollary 31: Any isometry of a Euclidean space E_n is an affine map.

Lemma 32 ([19, Proposition 9.7.1, restated]): For two sets $\{a_i\}_{i \in [k]}, \{b_i\}_{i \in [k]} \subset E_n$, $k \in \mathbb{N}$, where

$$\|a_i - a_j\|_2 = \|b_i - b_j\|_2, \quad \forall i, j \in [k], \quad (77)$$

there exists an isometry $\varphi \in \text{Isom}(E_n)$ such that $\varphi(a_i) = b_i$.

Theorem 33 (Krein-Milman Theorem [19, Theorem 11.6.8, restated]): For a compact convex set $\mathcal{S} \subset \mathbb{R}^n$,

$$\mathcal{S} = \text{conv}(\text{Extr}(\mathcal{S})). \quad (78)$$

Corollary 34: Let $\mathcal{P} \subset \mathbb{R}^n$ be a polytope with the set of vertices $\mathcal{V} = \{\mathbf{v}_i\}_{i \in [m]}$. Then $\mathbf{x} \in \mathcal{P} \setminus \mathcal{V}$ if, and only if, there exist $\{t_i\}_{i \in [m]}$, satisfying

$$0 \leq t_i < 1, \quad \forall i \in [m], \quad (79a)$$

$$\sum_{i \in [m]} t_i = 1, \quad (79b)$$

such that

$$\mathbf{x} = \sum_{i \in [m]} t_i \mathbf{v}_i. \quad (80)$$

Proof: This follows directly from Definition 20 and Theorem 33 (Krein-Milman Theorem). ■

Proposition 35: Let \mathcal{P} be a polytope in \mathbb{R}^n with \mathcal{V} being its set of vertices. Then for any $\alpha \in \text{Sym}_{E_n}(\mathcal{P})$,

$$\alpha(\mathcal{V}) = \mathcal{V}. \quad (81)$$

Proof: Let $\mathcal{V} = \{\mathbf{v}_i\}_{i \in [m]}$. From Corollary 34 we know that any $\mathbf{x} \in \mathcal{P} \setminus \mathcal{V}$ can be written as in (80) for some $\{t_i\}_{i \in [m]}$ satisfying (79). And from Corollary 31 and Definition 15 we know that any $\alpha \in \text{Sym}_{E_n}(\mathcal{P})$ is an affine map. Combining this we obtain

$$\alpha(\mathbf{x}) = \sum_{i \in [m]} t_i \alpha(\mathbf{v}_i), \quad (82)$$

proving that $\alpha(\mathbf{x}) \in \mathcal{P} \setminus \mathcal{V}$. Thus, we have shown that for any $\alpha \in \text{Sym}_{E_n}(\mathcal{P})$,

$$\left(\mathbf{x} \in \mathcal{P} \setminus \mathcal{V} \right) \implies \left(\alpha(\mathbf{x}) \in \mathcal{P} \setminus \mathcal{V} \right). \quad (83)$$

By implication this then means that for $\mathbf{y} \in \mathcal{P}$, $\alpha(\mathbf{y}) \in \mathcal{V}$ only if $\mathbf{y} \in \mathcal{V}$.

To show that $\alpha(\mathcal{V}) = \mathcal{V}$, we are thus only left to show that $\alpha(\mathbf{y}) \in \mathcal{V}$ if $\mathbf{y} \in \mathcal{V}$, which we will prove by contradiction. To proceed, first note that any isometry of E_n is bijective, and therefore the inverse map α^{-1} exists and $\alpha^{-1} \in \text{Sym}_{E_n}(\mathcal{P})$. Assume there exists $\mathbf{y} \in \mathcal{V}$ such that $\alpha(\mathbf{y}) \in \mathcal{P} \setminus \mathcal{V}$. This then yields that for $\mathbf{x} = \alpha(\mathbf{y}) \in \mathcal{P} \setminus \mathcal{V}$, $\alpha^{-1}(\mathbf{x}) = \mathbf{y} \in \mathcal{V}$, which contradicts (83). Thus $\mathbf{y} \in \mathcal{V} \implies \alpha(\mathbf{y}) \in \mathcal{V}$, concluding the proof. ■

B. Proof of Lemma 21

Applying Lemma 32, we know that for any $\mathbf{g} \in \text{G}_{\mathcal{V}(\mathcal{P})}$ there exists a (not necessarily unique) isometry $\alpha_g: E_n \rightarrow E_n$ satisfying $\alpha_g(\mathbf{x}_i) = \mathbf{g}\mathbf{x}_i$, $\forall \mathbf{x}_i \in \mathcal{V}(\mathcal{P})$. Moreover, from Corollary 31 we know that this isometry α_g is an affine map. In the following we make use of Definition 18 and the fact that \mathcal{P} is full-dimensional ($\dim \mathcal{P} = n$) in the embedding space \mathbb{R}^n to show that α_g is indeed the *unique* affine map (and also the unique isometry) satisfying $\alpha_g(\mathbf{x}_i) = \mathbf{g}\mathbf{x}_i$, $\forall \mathbf{x}_i \in \mathcal{V}(\mathcal{P})$. This is done by determining the map for $\mathbf{x} \in \mathbb{R}^n \setminus \mathcal{V}(\mathcal{P})$ by looking at the following two disjoint cases sequentially:

- 1) For $\mathbf{x} \in \mathcal{P} \setminus \mathcal{V}(\mathcal{P})$, we apply Corollary 34 and Definition 18 and obtain

$$\alpha_g(\mathbf{x}) = \alpha_g \left(\sum_{i \in [m]} t_i \mathbf{x}_i \right) = \sum_{i \in [m]} t_i \alpha_g(\mathbf{x}_i) \quad (84)$$

with $\{t_i\}_{i \in [m]}$ satisfying (79).¹⁰

- 2) For $\mathbf{x} \in \mathbb{R}^n \setminus \mathcal{P}$ and because $\dim \mathcal{P} = n$, there exists a unique $\mathbf{y} \in \partial \mathcal{P}$ (boundary of \mathcal{P}) and some scalar $r_{\mathbf{x}} > 1$ given by

$$r_{\mathbf{x}} \triangleq \inf\{\lambda > 0: \mathbf{x} \in \lambda \mathcal{P}\} \quad (85)$$

such that $\mathbf{x} = r_{\mathbf{x}} \mathbf{y}$. Since $\mathbf{y} \in \mathcal{P}$, $\alpha_g(\mathbf{y})$ is already well defined and due to Definition 18, we can thus write

$$\alpha_g(\mathbf{y}) = \alpha_g((1 - 1/r_{\mathbf{x}})\mathbf{0} + \mathbf{x}/r_{\mathbf{x}}) \quad (86)$$

$$= (1 - 1/r_{\mathbf{x}}) \alpha_g(\mathbf{0}) + \alpha_g(\mathbf{x})/r_{\mathbf{x}} \quad (87)$$

$$= \alpha_g(\mathbf{x})/r_{\mathbf{x}}, \quad (88)$$

$$\implies \alpha_g(\mathbf{x}) = r_{\mathbf{x}} \alpha_g(\mathbf{y}), \quad (89)$$

¹⁰Note that α_g is well defined even though there may exist $\{t'_i\}_{i \in [m]} \neq \{t_i\}_{i \in [m]}$ such that $\mathbf{x} = \sum_{i \in [m]} t'_i \mathbf{x}_i$.

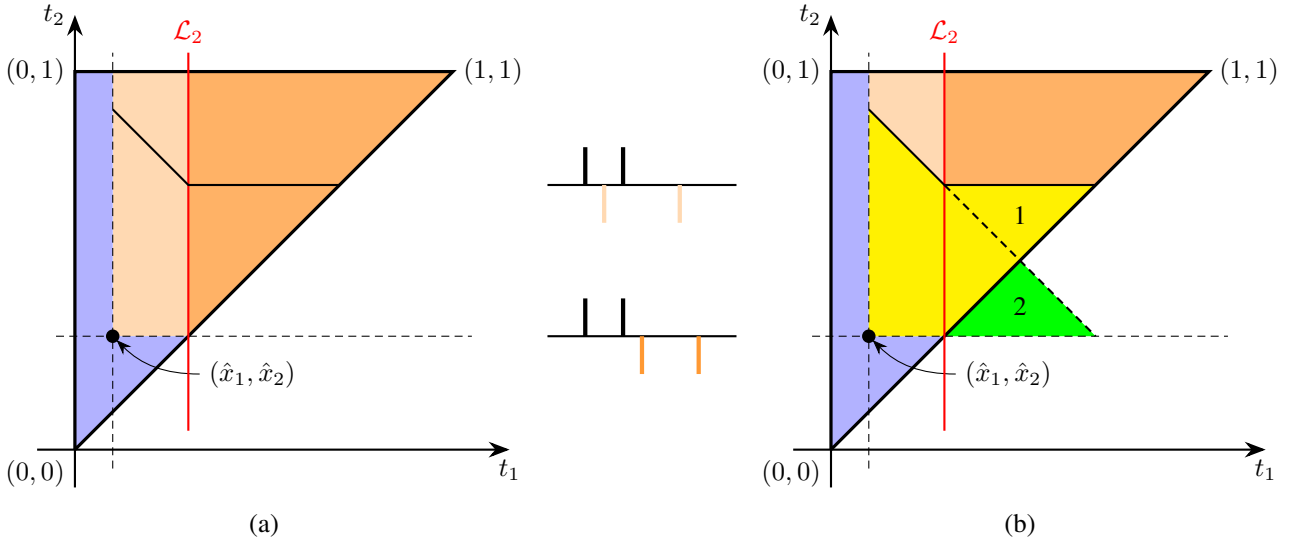


Fig. 4. In (a) the region where the distortion measure is finite, i.e., $\mathcal{R}_{d_q < \infty}(\hat{\mathbf{x}})$, is divided into the light orange region \mathcal{R}_1 and the dark orange region \mathcal{R}_2 by the vertical line $\mathcal{L}_2 \triangleq \{\mathbf{t} \in \mathbb{R}^2: t_1 = \hat{x}_2\}$. The black line depicts a contour line of constant distortion. The middle inset illustrates two different patterns of realizations of (t_1, t_2) from \mathcal{R}_1 and \mathcal{R}_2 in their respective color. The point pattern for (\hat{x}_1, \hat{x}_2) is illustrated in black. In (b) the distortion set $\mathcal{E}_{\hat{\mathbf{x}}}(D)$ as determined by the inequalities in (76) is shown in yellow. It has the same volume as DS_{σ_1} since replacing triangle 2 with triangle 1 preserves the volume.

where (88) holds because by (44)

$$\alpha_g(\mathbf{0}) = \alpha_g \left(\frac{1}{m} \sum_{i \in [m]} \mathbf{x}_i \right) = \frac{1}{m} \sum_{i \in [m]} \alpha_g(\mathbf{x}_i) = \mathbf{0}. \quad (90)$$

It only remains to justify (49) and (50).

To show (49), we first note that we have already shown that

$$f: G_{\mathcal{V}(\mathcal{P})} \rightarrow \text{Isom}(E_n), \quad g \mapsto \alpha_g \quad (91)$$

is well defined. Clearly f is one-to-one, and moreover $\alpha_g(\mathcal{P}) = \mathcal{P}, \forall g \in G_{\mathcal{V}(\mathcal{P})}$. Thus, from Definition 15, we obtain

$$\{\alpha_g: g \in G_{\mathcal{V}(\mathcal{P})}\} \subseteq \text{Sym}_{E_n}(\mathcal{P}). \quad (92)$$

On the other hand, applying Proposition 35 we get

$$\text{Sym}_{E_n}(\mathcal{P}) \subseteq \{\alpha \in \text{Isom}(E_n): \alpha(\mathcal{V}(\mathcal{P})) = \mathcal{V}(\mathcal{P})\} \quad (93)$$

$$= \{\alpha_g: g \in G_{\mathcal{V}(\mathcal{P})}\}. \quad (94)$$

Combining (92) and (94) we conclude that

$$\text{Sym}_{E_n}(\mathcal{P}) = \{\alpha_g: g \in G_{\mathcal{V}(\mathcal{P})}\}. \quad (95)$$

To show (50), we first rewrite (91) to be a bijection

$$f: G_{\mathcal{V}(\mathcal{P})} \rightarrow \text{Sym}_{E_n}(\mathcal{P}), \quad g \mapsto \alpha_g. \quad (96)$$

Thus we are left to show that f is a homomorphism, i.e., that for any $g', g \in G_{\mathcal{V}(\mathcal{P})}$,

$$f(g' \cdot g) = f(g') \circ f(g), \quad (97)$$

where ‘ \cdot ’ and ‘ \circ ’ are the group operations of $G_{\mathcal{V}(\mathcal{P})}$ and $\text{Sym}_{E_n}(\mathcal{P})$, respectively. To this goal, since (97) is equivalent to

$$\alpha_{g' \cdot g} = \alpha_{g'} \circ \alpha_g, \quad (98)$$

in the following we prove that (98) holds for all $\mathbf{x} \in \mathbb{R}^n$ by considering three disjoint cases sequentially:

(i) $\mathbf{x}_i \in \mathcal{V}(\mathcal{P})$:

$$\begin{aligned} \alpha_{g' \cdot g}(\mathbf{x}_i) &= (g' \cdot g) \mathbf{x}_i = g'(g \mathbf{x}_i) \\ &= \alpha_{g'}(\alpha_g(\mathbf{x}_i)) = (\alpha_{g'} \circ \alpha_g)(\mathbf{x}_i). \end{aligned} \quad (99)$$

(ii) $\mathbf{x} \in \mathcal{P} \setminus \mathcal{V}(\mathcal{P})$: Using (84) and (i):

$$\alpha_{g' \cdot g}(\mathbf{x}) = \alpha_{g' \cdot g} \left(\sum_{i \in [m]} t_i \mathbf{x}_i \right) \quad (100)$$

$$= \sum_{i \in [m]} t_i \alpha_{g' \cdot g}(\mathbf{x}_i) \quad (\text{by (84)}) \quad (101)$$

$$= \sum_{i \in [m]} t_i (\alpha_{g'} \circ \alpha_g)(\mathbf{x}_i) \quad (\text{by (i)}) \quad (102)$$

$$= (\alpha_{g'} \circ \alpha_g) \left(\sum_{i \in [m]} t_i \mathbf{x}_i \right) \quad (103)$$

$$= (\alpha_{g'} \circ \alpha_g)(\mathbf{x}). \quad (104)$$

(iii) $\mathbf{x} \in \mathbb{R}^n \setminus \mathcal{P}$: Using (89) and $\mathbf{x} = r_{\mathbf{x}} \mathbf{y}$ where $\mathbf{y} \in \partial \mathcal{P}$, and noting that from (i) and (ii) we have $\alpha_{g' \cdot g}(\mathbf{y}) = (\alpha_{g'} \circ \alpha_g)(\mathbf{y})$, we obtain

$$\begin{aligned} \alpha_{g' \cdot g}(\mathbf{x}) &= r_{\mathbf{x}} \alpha_{g' \cdot g}(\mathbf{y}) \\ &= r_{\mathbf{x}} (\alpha_{g'} \circ \alpha_g)(\mathbf{y}) = (\alpha_{g'} \circ \alpha_g)(\mathbf{x}). \end{aligned} \quad (105)$$

From the Cases (i)–(iii) we conclude that $\alpha_{g' \cdot g}(\mathbf{x}) = (\alpha_{g'} \circ \alpha_g)(\mathbf{x}), \forall \mathbf{x} \in \mathbb{R}^n$, and that therefore (98) holds. In combination with the bijective map f in (96) this means that f is an isomorphism and thus $\text{Sym}_{E_n}(\mathcal{P}) \cong G_{\mathcal{V}(\mathcal{P})}$.

APPENDIX C

PROOF OF THEOREM 27

A. Preliminaries for the Proof

Definition 36 (Path and Path Length): A path $\mathbf{p} = v_0 v_1 \cdots v_k$ in a graph $\Gamma = (\mathbf{V}, \mathbf{E})$ is a sequence of distinct

vertices where $v_i \in V$ and $\{v_{i-1}, v_i\} \in E$, $\forall i \in [k]$. We say that p is a path between v_0 and v_k .

The *length* of a path p is the number of edges it consists of, and we denote it as $|p| = k$. Two distinct vertices v and v' are *linked* if there is a path between them; and a path linking v and v' with the minimal length is called a *shortest path* between v and v' .

For two linked vertices $v \neq v'$ in graph Γ , the length of the shortest path between them is denoted by $l_\Gamma(v, v')$.

Proposition 37: For $v, v', w, w' \in \mathcal{V}(\square^n)$, $v \neq v'$, $w \neq w'$,

$$\begin{aligned} \|v - v'\|_2 = \|w - w'\|_2 \\ \iff l_{\Gamma_{\square^n}}(v, v') = l_{\Gamma_{\square^n}}(w, w'). \end{aligned} \quad (106)$$

Note that any two distinct vertices of Γ_{\square^n} are linked, and therefore the length of the shortest path is always well defined here.

Proof: This follows immediately from the fact that the Hamming distance between two vertices of \square^n is equal to k if, and only if, their ℓ_2 -distance is \sqrt{k} . ■

Lemma 38: For any $\varphi \in \text{Aut}(\Gamma_{\square^n})$, $v, v' \in \mathcal{V}(\square^n)$,

$$\|v - v'\|_2 = \|\varphi(v) - \varphi(v')\|_2. \quad (107)$$

Proof: For $v = v'$, the proposition clearly holds. For any $v \neq v'$, first note that because $\varphi \in \text{Aut}(\Gamma_{\square^n})$, any length- k path $p = vv_1 \cdots v_{k-1}v'$ between v and v' in Γ_{\square^n} can be bijectively mapped to the length- k path $\tilde{p} = \varphi(v)\varphi(v_1) \cdots \varphi(v_{k-1})\varphi(v')$ between $\varphi(v)$ and $\varphi(v')$ in Γ_{\square^n} . This holds for any k and thus we have:

$$l_{\Gamma_{\square^n}}(v, v') = l_{\Gamma_{\square^n}}(\varphi(v), \varphi(v')). \quad (108)$$

Using (108) and Proposition 37 we get

$$\|v - v'\|_2 = \|\varphi(v) - \varphi(v')\|_2, \quad (109)$$

which concludes the proof. ■

Corollary 39: Let $\Gamma_{\square^n} = (V, E)$. Then for a bijection $\varphi : V \rightarrow V, v \mapsto \varphi(v)$, the following holds: $\varphi \in \text{Aut}(\Gamma_{\square^n})$ if, and only if,

$$\|v - v'\|_2 = \|\varphi(v) - \varphi(v')\|_2, \quad \forall v, v' \in V. \quad (110)$$

Proof: The only-if part follows directly from Lemma 38. To show that (110) implies $\varphi \in \text{Aut}(\Gamma_{\square^n})$, we first note that from the definition of Γ_{\square^n} we have

$$\{v, v'\} \in E \iff \|v - v'\|_2 = 1. \quad (111)$$

Thus, by (110),

$$\{v, v'\} \in E \iff \|\varphi(v) - \varphi(v')\|_2 = 1 \quad (112)$$

$$\iff \{\varphi(v), \varphi(v')\} \in E \quad \forall v, v' \in V, \quad (113)$$

which means that $\varphi \in \text{Aut}(\Gamma_{\square^n})$. ■

B. Proof of Theorem 27

Using Corollary 39, we can write

$$\begin{aligned} \text{Aut}(\Gamma_{\square^n}) \\ \cong \{g \in S_{2^n} : \|v - v'\|_2 = \|gv - gv'\|_2, \forall v, v' \in \mathcal{V}(\square^n)\} \end{aligned} \quad (114)$$

$$= G_{\mathcal{V}(\square^n)}. \quad (115)$$

Furthermore, applying Lemma 21, we have

$$\text{Sym}_{E_n}(\square^n) \cong G_{\mathcal{V}(\square^n)}, \quad (116)$$

and combining this with (115) we finally get

$$\text{Sym}_{E_n}(\square^n) \cong \text{Aut}(\Gamma_{\square^n}), \quad (117)$$

concluding the proof.

REFERENCES

- [1] H.-A. Shen, S. M. Moser, and J.-P. Pfister, "Sphere covering for Poisson processes," in *Proc. 2020 IEEE Inf. Theory Workshop*, Riva del Garda, Italy, Apr. 11–15, 2021, pp. 181–185.
- [2] A. Lapidoto, A. Malär, and L. Wang, "Covering point patterns," in *Proc. IEEE Int. Symp. Inf. Theory*, St. Petersburg, Russia, Jul. 31 – Aug. 5, 2011, pp. 51–55.
- [3] —, "Covering point patterns," *IEEE Trans. Inf. Theory*, vol. 61, no. 9, pp. 4521–4533, Sept. 2011.
- [4] T. P. Coleman, N. Kiyavash, and V. G. Subramanian, "The rate-distortion function of a Poisson process with a queueing distortion measure," in *Proc. Data Compression Conf.*, Snowbird, UT, USA, Mar. 25–27, 2008, pp. 63–72.
- [5] I. Rubin, "Rate-distortion functions for nonhomogeneous Poisson processes," *IEEE Trans. Inf. Theory*, vol. 20, no. 5, pp. 669–672, Sept. 1974.
- [6] —, "Information rates and data-compression schemes for Poisson processes," *IEEE Trans. Inf. Theory*, vol. 20, no. 2, pp. 200–210, Mar. 1974.
- [7] —, "Information rates for Poisson sequences," *IEEE Trans. Inf. Theory*, vol. 19, no. 3, pp. 283–294, May 1973.
- [8] N. V. Shende and A. B. Wagner, "Functional covering of point processes," in *Proc. IEEE Int. Symp. Inf. Theory*, Paris, France, Jul. 7–12, 2019, pp. 2039–2043.
- [9] A. Mazumdar and L. Wang, "Covering arbitrary point patterns," in *Proc. 50th Allerton Conf. Commun., Control Comput.*, Monticello, IL, USA, Oct. 1–5, 2012, pp. 2075–2080.
- [10] H. Si, O. O. Koyluoglu, and S. Vishwanath, "Lossy compression of exponential and Laplacian sources using expansion coding," in *Proc. IEEE Int. Symp. Inf. Theory*, Honolulu, HI, USA, Jun. 29 – Jul. 4, 2014, pp. 3052–3056.
- [11] M. Baake, "Structure and representations of the hyperoctahedral group," *J. Math. Physics*, vol. 25, no. 11, pp. 3171–3182, Nov. 1984.
- [12] J. J. Rotman, *An Introduction to the Theory of Groups*, 4th ed. New York, USA: Springer Verlag, 1995.
- [13] R. Diestel, *Graph Theory*, 5th ed. Berlin, Germany: Springer Verlag, 2017.
- [14] P. Gregor, *Hypercube Structures (Lecture)*, Charles University, Prague, Czech Republic, 2020. [Online]. Available: <https://ktiml.mff.cuni.cz/~gregor/hypercube/hypercube-course.htm>
- [15] F. Harary, "The automorphism group of a hypercube," *J. Univ. Comp. Sc.*, vol. 6, no. 1, pp. 136–138, Jan. 2000.
- [16] R. Frucht, "Herstellung von Graphen mit vorgegebener abstrakter Gruppe," *Compositio Math.*, vol. 6, pp. 239–250, 1939.
- [17] S. Mazur and S. Ulam, "Sur les transformations isométriques d'espaces vectoriels normés," *C. r. hebd. des séances Acad. sci.*, vol. 194, pp. 946–948, 1932.
- [18] P. D. Lax, *Functional Analysis*, ser. Wiley Series in Pure and Applied Mathematics. New York, USA: Wiley, 2002.
- [19] M. Berger, *Geometry I*. New York, USA: Springer Verlag, 1987, translated from French by M. Cole and S. Levy.